Modelling cyclists' comfort zones from obstacle avoidance manoeuvres

Lee, Oliver; Rasch, Alexander; Schwab, Arend L.; Dozza, Marco

Important note
To cite this publication, please use the final published version (if applicable).
Please check the document version above.

Modelling cyclists' comfort zones from obstacle avoidance manoeuvres

Oliver Lee[a], Alexander Rasch[b], Arend L. Schwab[a,*], Marco Dozza[b]

[a] *Delft University of Technology, the Netherlands*
[b] *Chalmers University of Technology, Sweden*

A B S T R A C T

This paper introduces a framework for modelling the cyclist's comfort zone. Unlike the driver's comfort zone, little is known about the cyclist's. The framework draws on existing literature in cognitive science about driver behaviour to explain experimental results from cycling field trials, and the modelling of these results. We modelled braking and steering manoeuvres from field data of cyclists' obstacle avoidance within their comfort zone. Results show that when cyclists avoided obstacles by braking, they kept a constant deceleration; as speed increased, they started to brake earlier, farther from the obstacle, maintaining an almost constant time to collision. When cyclists avoided obstacles by steering, they maintained a constant distance from the object, independent of speed. Overall, the higher the speed, the more the steering manoeuvres were temporally delayed compared to braking manoeuvres. We discuss these results and other similarities between cyclist and driver behaviour during obstacle avoidance. Implications for the design of acceptable active safety and infrastructure design are also addressed.

1. Introduction

In several countries worldwide, cycling is increasingly popular, raising new safety concerns (Dozza et al., 2018). The—still-controversial—safety-in-numbers mechanism (Bhatia and Wier, 2011; Elvik, 2009; Johnson et al., 2010) predicts that the number of crashes will not increase proportionally with the number of cyclists. However, more cyclists may result in more crowded infrastructure, increasing the number and severity of conflicts between motorised vehicles and cyclists (Dozza and Bianchi-Piccinini, 2014).

Cycling safety is an old issue (Brezina and Krämer, 1970; Hudson, 1978), which can be addressed by improving the infrastructure and, more recently, with active safety systems (i.e. intelligent systems which are typically installed on motorised vehicles). These systems leverage technology to recognise dangerous situations and take action before they devolve into crashes, per SAE J3063, SAE International, 2015). Both active safety and infrastructure design may address cyclist behaviour by predicting the space and time that a cyclist may need to avoid an obstacle (Gustafsson et al., 2013; Schepers et al., 2017). For instance, when a driver and a cyclist negotiate an intersection, active safety systems must predict whether the cyclist intends to brake or not to choose the safest intervention strategy. An active safety system may assume the space and time necessary for comfort braking as a basis to infer whether the cyclist plans to pass before the driver or to yield at the intersection. Similarly to active safety design, infrastructure design may

consider the cyclists' needs for comfortable manoeuvring to prevent safety-critical situations that may result into a crash. For instance, the width of a bicycle path should comply with cyclists' needs for comfortable steering to make overtaking safe (Schwab and Meijaard, 2017). Thus, it becomes essential to understand how cyclists brake and steer during *comfortable manoeuvring* (as a part of the usual cycling experience), and not just in safety-critical situations where immediate and extreme actions may be required.

In the early 20th century, Gibson and Crooks were among the first cognitive scientists interested in how humans manoeuvre to prevent collisions (Gibson and Crooks, 1938). Gibson and Crooks introduced the concept of *field of safe travel to the minimum stopping zone* (the estimated braking distance necessary to come to a halt). Gibson and Crooks envisioned the field of safe travel as a space, shaped by the presence of the obstacles that the driver must avoid to complete her journey safely and on the vehicle's limitations for steering and braking. For instance, the concept of minimum stopping zone was introduced for drivers to highlight the space margin needed to reduce a car's speed to zero. Similarly to drivers, cyclists have their field of safe travel and minimum stopping zone, and this paper is a first attempt to measure and operationalise these concepts for cycling safety. Since 1938, many authors built on the concept of field of safe travel: relating it to risk, introducing new ideas such as *safety margins* and *comfort zone*, and contributing new cognitive (theoretical) models to explain how internal and external motivations may shape the field of safe travel (Damasio and Damasio,

---

1995; Fuller, 1984; Näätänen and Summala, 1974; Summala, 2007; Vaa, 2014). Because both drivers and cyclists are humans operating a vehicle, many of the concepts and models developed for driver behaviour may be adapted to cyclist behaviour and help explain the motivation and the results of this paper. Particularly noteworthy is the concept of comfort zone (Vaa, 2014), which has been primarily investigated for drivers (Bärgman, 2016), less investigated for pedestrians (Lübbe, 2015) and still poorly studied for cyclists (Boda, 2019).

Understanding the specific capabilities of bicycles becomes crucial to investigate cycling manoeuvres and frame cyclist's comfort zone within the operational design domain of a bicycle. In fact, bicycle dynamics set objective constraints for how cyclists may experience and adapt their comfort zones, and may explain some difference between drivers' and cyclists' comfort zones. Whereas drivers only have to manoeuvre the vehicle, cyclists must also balance the vehicle. With only two contact points on the ground, the bicycle is a laterally unstable vehicle, and some lateral space is necessary to maintain balance. Cars usually need less lateral space at lower speeds; however, the opposite is true for bicycles, because of a steer-into-the-fall balance mechanism (Kooiman et al., 2011, Schwab and Meijaard, 2017). Additionally, the countersteering mechanism (i.e. the rider has to steer briefly to the left to make the bicycle fall into a right turn, and vice versa) results in bicycles needing more lateral space to turn at lower speeds (Schwab and Meijaard, 2013) when compared to cars. Therefore, bicycle stability and manoeuvrability constrain both the minimum stopping distance and the overall field of safe travel.

The objective of this paper is to define, measure, and model the cyclist's comfort zone for avoidance manoeuvres involving braking or steering. In other words, the research question we address is: "how can we quantify and model cyclist comfortable manoeuvring to support active safety and infrastructure design?". The models presented in this paper can inform infrastructure design and improve active safety systems by integrating models of cyclist behaviour into the algorithms for threat assessment and decision making (Brannstrom et al., 2010; Brännström et al., 2014). In fact, these algorithms continuously predict road-users' behaviour to estimate the probability of a conflict (threat assessment) and determine which intervention, if any, is needed (decision making). However, a foundation for threat assessment and decision making is the availability of a cyclist steering and braking model.

This paper also serves as a bridge between driver behaviour and cyclist behaviour research, making use of the former to define, measure, and explain comfort zones for the latter. In addition, this paper helps operationalising the concept of the cyclist comfort zone for its application to the design of solutions which increase cycling safety.

2. Method

2.1. Participants

Eighteen participants were recruited from the Gothenburg area and asked to ride a bicycle while performing braking or steering avoidance manoeuvres at different speeds. Inclusion criteria required participants to be within the ages of 20 to 35 years (to limit the effect of age on our results), cycle at least once a week (weather permitting, according to self-reported information from the participants), have experience with a coaster brake (i.e. a rear-wheel hub brake operated by pedalling backwards, common in some European countries such as Sweden and the Netherlands), and have a height of at least 165 cm (to ride the instrumented bicycle comfortably). The experiment required the participants to either brake or steer in different conditions to *comfortably* avoid a stationary dummy cyclist. The data from two of the participants were excluded from analysis (because of recording issues or because the participants did not follow the experimental protocol). The ages of the remaining participants, 12 males and four females, ranged from 20 to 35 years (mean = 25.9, std = 2.2). Participants reported they cycled on average 5.5 h per week (std = 3.3). As their motivation for cycling, four

Fig. 1. Instrumented bicycle: a classic urban 3-speed bicycle with a step-through frame, a rear coaster brake, and a drum brake on the front wheel; the instrumentation, powered by a power bank, comprises an angle sensor, an inertial measurement unit, a speed sensor, and a logger.

participants cited sport, three recreation, four touring, and 16 commuting.

2.2. Data collection

Two separate data logging platforms colleted data: an instrumented bicycle and a stationary LIDAR.

2.2.1. Instrumented bicycle

The instrumented bicycle was a classic urban 3-speed bicycle with a step-through frame, a rear coaster brake, and a drum brake on the front wheel; see Fig. 1. The bicycle logging platform ran a C program on a Raspberry Pi 3 Model B. Data were collected from an inertial measurement unit (IMU; PhidgetSpatial Precision 3/3/3 1044), a potentiometer to measure steer angle, a DC motor to measure velocity, and a push button for synchronisation with the other logging platform (in post-processing). The IMU measured acceleration within a range of ± 2 g, angular rate within a range of ± 400 deg/s for two of the orthogonal axes and ± 300 deg/s for the third axis, and magnetic field within a range of 0–5.5 G. The IMU was rigidly attached to the rear rack of the bicycle, oriented with the positive x-axis in the direction of the bicycle motion and the positive y-axis parallel to gravity and pointing down. In order to measure the handlebar steer angle, a potentiometer was connected with a belt system to the bicycle stem and configured such that ± 60 deg spanned 0–5 V. A direct-current motor, mounted inside a bottle dynamo, engaged the rear tire and worked as a speed sensor. The sensors were sampled at 125 Hz, and analogue values were digitised by a 10-bit ADC (MCP3008). The logging platform was mounted to a typical city bike (Fig. 1). The bicycle was also equipped with a speedometer which the participants used to gauge their speed. The speedometer, which was used to calibrate the speed output by the speed sensor, was not recorded.

2.2.2. Stationary LIDAR

The LIDAR logging platform was implemented as a ROS package written in Python and run on a second Raspberry Pi 3 Model B. Data were collected from a scanning LIDAR (Hokuyo UXM-30LXH-EWA) and a push-button permitted synchronisation with the other logging platform. The LIDAR had a guaranteed detection range of 30 m, a scanning angle of 190 deg, and an angle step of 0.125 deg. Data were sampled at 20 Hz. The two logging platforms were synchronised by cross-correlating the timestamps of each platform after upsampling the LIDAR signals to 125 Hz.
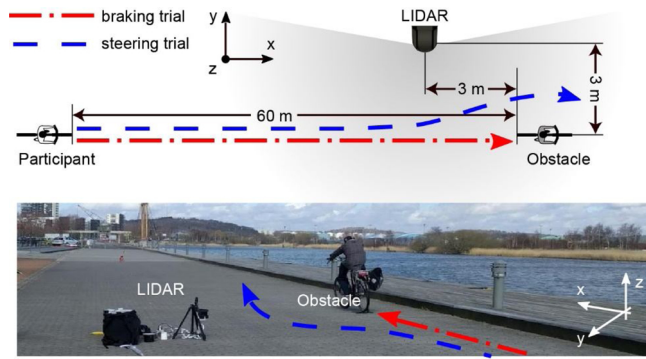
Fig. 2. Experiment setup with the instrumented bicycle, static obstacle, and LIDAR.

Fig. 3. Comparison of the velocity measured from the speed sensor with the velocity obtained from the Kalman smoother in one representative trial. The measured acceleration, used to determine the start and stop of the braking event, is also shown.

2.3. Experimental protocol

During the experiment, the participants were asked to ride the instrumented bicycle on a straight path toward the dummy cyclist, which was placed 60 m ahead (Fig. 2). The LIDAR was placed close to the dummy to record the manoeuvres of the participants as they approached and avoided the dummy, either by steering or braking. The LIDAR was mounted on a tripod 0.3 m above the ground (the same height as the hub of the instrumented bicycle wheels).

Before starting the experiment, participants were given time to get familiar with the dynamics and control of the instrumented bicycle. They practised braking, steering, and maintaining specific speeds (by monitoring the speedometer mounted on the handlebar) until they felt comfortable performing the experiment. For each trial, the participant was instructed what speed to maintain (one of three different speed representative of three different stability levels: laterally unstable, 12 km/h; self-stable, 17 km/h; and mildly unstable, 22 km/h; Meijaard et al. (2007) and what manoeuvre to perform (braking or steering). Participants were asked to brake or steer comfortably as they would do in traffic. The only requirement was for the participant to come to a complete stop before the dummy for braking manoeuvres, and to overtake the dummy for steering manoeuvres. Each participant performed 18 trials (three braking and three steering manoeuvres for each of the three speeds). The trials took place in blocks of three: the participant cycled at each of the three speeds in one block, in an order given by the instructor. The order of speeds was predetermined from a list of all possible combinations to appear random to the participant. The avoidance method was alternated in each trial block. These measures were taken to minimise, and control for, motor learning during the experiment.

2.4. Data processing

The measurement data were processed to obtain metrics to create braking and steering models describing each cyclist's comfort zone. Specifically, we calculated distance-to-collision (DTC) and time-to-collision (TTC) at the onset of all manoeuvres. We also computed deceleration during braking manoeuvres. For the steering manoeuvres, we calculated the lateral clearance to the dummy and the duration and longitudinal space required by the manoeuvre.

2.4.1. Speed reconstruction and trajectory estimation

Because speed was not available from the speed sensor for most trials (due to a technical failure), cyclist velocity was estimated from the LIDAR data. This estimation used a Rauch-Tung-Striebel smoother, which included an extended Kalman filter with a constant turn rate and a constant-acceleration motion model. This model also estimated the position of the cyclist's centroid, which we later used to determine braking distance and lateral clearance. The speed signal from the speed
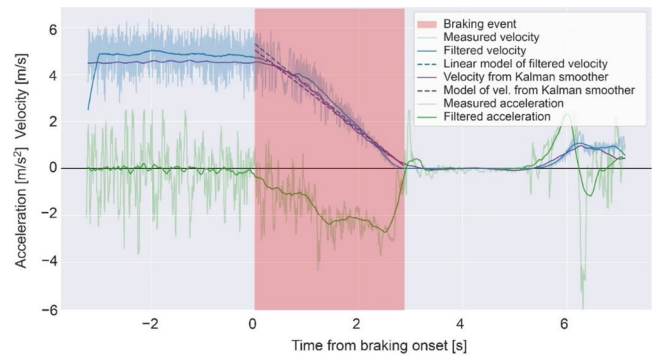
sensor was available for eight trials, so we used these trials to tune the Kalman smoother and verify its accuracy. One of these eight trials, showing measured and estimated velocities, is shown in Fig. 3.

2.4.2. Manoeuvre identification

The braking manoeuvre was identified as the largest contiguous region of acceleration data above 0.3 m/s^2. Small subregions (less than 0.6 s) below the threshold were ignored when calculating a contiguous region.

The overtaking manoeuvre was determined from the cyclist's trajectory. The start of the overtaking event was determined by the first local maximum in the trajectory (lateral displacement) in front of the obstacle. The end of the overtaking event was defined as the point at which the cyclist returned to the lateral displacement of the start point (Fig. 4).

2.4.3. Distance-to-collision, time-to-collision, and lateral clearance

The DTC, calculated from the LIDAR point cloud, was defined as the distance from the frontmost point of the front wheel of the rider to the rearmost point of the rear wheel of the obstacle at the start of the avoidance manoeuvre. The TTC was defined as the ratio of DTC to speed at the start of the avoidance manoeuvre. Lateral clearance was also calculated from the point cloud as the minimum point-to-point distance from the cyclist to the obstacle clusters during the overtaking manoeuvre. We also calculated the duration of all avoidance manoeuvres and the braking distance (for braking manoeuvres).

2.4.4. Statistical analysis and modelling

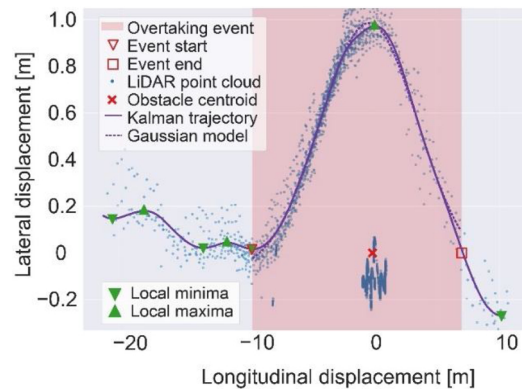Braking was modelled as a constant deceleration by applying a

Fig. 4. The trajectory from Kalman smoother and Gaussian model fit in one representative steering trial. The identification of the steering event from the path curvature is also shown.

linear regression model to the speed. The model's goodness of fit was evaluated by calculating the normalised root-mean-square deviation. For steering manoeuvres, we modelled the trajectory of the cyclist's centroid as a Gaussian curve and parameterised it according to the longitudinal distance of the overtaking manoeuvre x (distance tail to tail) and the lateral distance y from the obstacle (amplitude of the Gaussian curve) with the form

$$y = a\, e^{-\frac{(x-\mu)^2}{2\sigma^2}} + b, \tag{1}$$

where a is the Gaussian amplitude, b is the Gaussian y-intercept, μ is the Gaussian mean, and σ is the Gaussian standard deviation. A Gaussian curve was chosen since the tails capture the complete manoeuvre better than a partial wave, and it requires fewer parameters than a piecewise cubic spline. Correlation analyses assessed the extent to which DTC, TTC, manoeuvre durations, braking distance, and lateral clearance were affected by speed. T-tests verified whether DTC and TTC differed between steering and braking manoeuvres.

3. Results

Overall, 286 trials from 16 riders were used to analyse and model comfortable braking and steering. Overall results are presented in Table 1. Steering manoeuvres were initiated at slightly shorter DTC and TTC than braking manoeuvres. Paired t-tests verified that these results were statistically significant (p < 0.05). As speed increased, the differences between braking and steering in terms of DTC and TTC became more evident (Fig. 5). The duration of braking manoeuvres increased as speed increased (r = 0.27), while the duration of steering manoeuvres decreased as speed increased (r = −0.53; Fig. 5). Consequently, as speed increased, steering manoeuvres became faster than braking manoeuvres.

3.1. Braking

The higher the speed, the larger the DTC (the range of the Pearson coefficient across participants was r = 0.61 to 0.97, median r = 0.93). Half of the subjects maintained similar deceleration profiles (obtained from the linear model) across the different speed conditions (r < 0.6), and only three participants braked significantly harder as speed increased (r > 0.8). This suggests that most cyclists compensated for the higher speeds by braking earlier so that the braking distance increased with speed (Table 2) rather than by braking harder. This result is supported by the low correlation between speed and TTC (the range of the Pearson coefficient across participants was r = −0.68 to 0.93, median r = 0.47). Because of the few participants who did brake harder as speed increased, the average deceleration across participants increased slightly with speed (Table 2). The overall Pearson coefficient between speed and deceleration was r = 0.74. (The goodness of fit for the deceleration from the linear model was verified by calculating the normalised root-mean-square deviation, which had an average of 0.073 m/s and a standard deviation of 0.035 m/s.) Fig. 6 shows the individual speed profiles and coefficients from the linear models (decelerations) for each participant in order of braking intensity. In other words, the top-left panel of Fig. 6 shows the participant who braked the hardest (and started braking latest) whereas the bottom-right panel shows the participant who braked the mildest (and started braking

earliest). The variability across participants is relatively large as the hardest brake was four times larger than the mildest. It is evident from our model that braking manoeuvres were more similar within the same cyclist than among different cyclists (Fig. 6). Furthermore, the higher the deceleration, the more consistent were the cyclists across braking manoeuvre (this is particularly evident for the four subjects in the first row of panels in Fig. 6).

3.2. Steering

As speed increased, steering manoeuvres occurred at slightly larger DTCs (the range of the Pearson coefficient across participants was r = −0.22 to 0.76, median r = 0.33) and significantly shorter TTCs (the range of the Pearson coefficient across participants was r = −0.73 to −0.09, median r = −0.53). Interestingly, for braking, the starting velocity was more correlated to DTC than to TTC, whereas for steering, we found the opposite result. Minimum clearance was not consistently correlated with speed across subjects (r = −0.62 to 0.81, median = 0.23; Table 3) and with the longitudinal distance covered during the overtaking manoeuvre (−0.55 to 0.94, median = 0.52). Fig. 7 shows the individual steering manoeuvres, their models, and the parameters of the models. The maximum lateral passing distance was similar across all participants and was reached −1.5 to 1.5 m from the dummy cyclist (μ parameter in the model; Fig. 7). The σ parameter of the model was between 2.8 m and 5.6 m, indicating that, at such distance from the dummy, all cyclist had already entered the steer-away phase of the overtaking (Dozza et al., 2016). The amplitude of the Gaussian model (parameter a) ranged 0.9–1.5 m, indicating that the lateral clearance from the model was 0.6-0.9 m (after subtracting half of the dummy cyclist width). Finally, the position of the cyclist within the lane as she approaches the dummy is evident from the b parameter, that shows differences as large as 0.7 m across participants. (Because the obstacle was 60 cm wide, all cyclists were on a collision course from the start of the steering manoeuvre; in fact, b was within −0.3 m and 0.4 m).

4. Discussion

In this paper, cyclist braking was described with a constant deceleration model and cyclist steering with a Gaussian curve model. A total of 142 braking trials and 144 steering trials contributed to the models (because of an instructor error two braking trials were lost). The two models capture the main features of comfortable braking and steering in planned obstacle avoidance. These models fill a gap in the literature by quantifying, for the first time, cyclist comfort zones in common scenarios: when 1) braking to reach a full stop within a specific distance, such as when approaching an intersection with a red light or 2) steering to avoid an obstacle, such as overtaking another cyclist.

For braking, deceleration seemed to be the predominant consideration. We found that cyclists generally execute comfortable braking by keeping their deceleration constant. Individual deceleration preference varied from 0.6 to 2.4 m/s², and the variability across individuals was much larger than the variability within individuals across speeds. Interestingly, the larger the deceleration, the lower the variability. This finding is consistent with previous literature on driver comfort zones, showing that deceleration is an important, and individual, aspect of drivers' comfort levels (Bärgman et al., 2015). This result also suggests that an active safety system may assume that a cyclist approaching an intersection will continue braking with the same deceleration once she has started braking, and with a greater likelihood for larger deceleration. This result also suggests that threat assessment algorithms should not expect for a cyclist to decelerate more than 2.4 m/s², because such a large deceleration may not be comfortable even for the most aggressive cyclists. Future studies may highlight which subjective characteristics (e.g., demographics and personality traits) and which environmental factors (e.g., ice on the road, poor

Table 1
Overall time-to-collision, distance-to-collision, and duration for braking and steering manoeuvres (mean ± standard deviation).

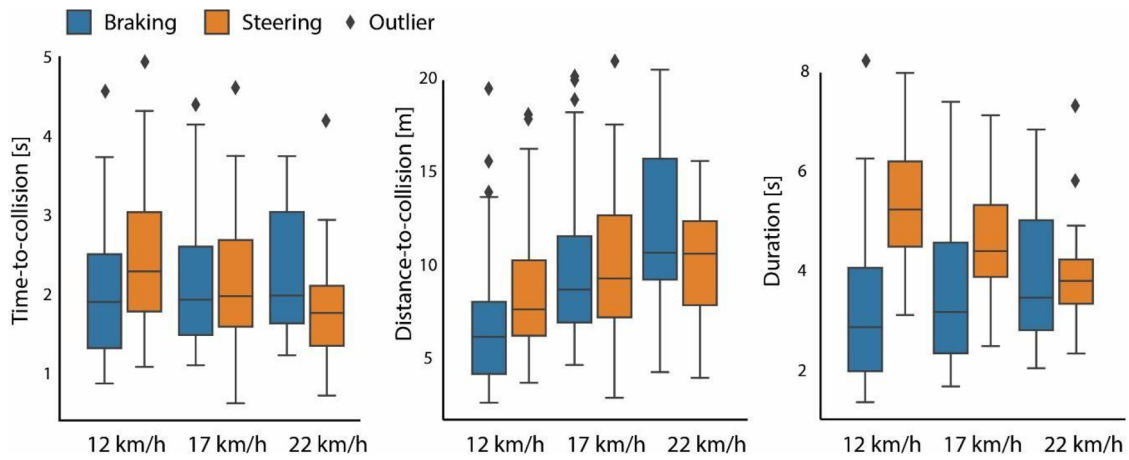| Manoeuvre	Time-to-Collision [s]	Distance-to-Collision [m]	Duration [s]
Braking	2.16 ± 0.82	9.65 ± 4.66	3.57 ± 1.45
Steering	2.12 ± 0.85	9.51 ± 3.64	4.63 ± 1.20

Fig. 5. Time-to-collision, distance-to-collision, and duration for braking and steering manoeuvres.

Table 2
Distance, duration, and calculated deceleration for the braking manoeuvres at the three speeds, together with the averaged values and starndard deviations.

Speed [km/h]	Distance [m]	Duration [s]	Deceleration [m/s^2]
12	3.13 ± 1.38	5.31 ± 2.54	1.31 ± 0.59
17	3.64 ± 1.52	8.32 ± 3.73	1.56 ± 0.64
22	3.92 ± 1.36	11.37 ± 4.57	1.73 ± 0.60
Overall averaged	3.57 ± 1.45	8.35 ± 4.44	1.53 ± 0.63

Table 3
Distance, duration, and clearance for the overall steering manoeuvres at the three speeds, together with the averaged values and standard deviations.

Speed [km/h]	Distance [m]	Duration [s]	Clearance [m]
12	18.14 ± 3.96	5.48 ± 1.19	0.86 ± 0.19
17	20.68 ± 4.62	4.58 ± 1.03	0.88 ± 0.17
22	21.74 ± 4.05	3.81 ± 0.68	0.90 ± 0.17
Overall averaged	20.17 ± 4.46	4.63 ± 1.20	0.88 ± 0.17

visibility) may impact comfortable deceleration and possibly help active safety systems assume an even lower threshold (than 2.4 m/s^2) for cyclist braking. In fact, previous literature points out that females (who were a minority in our study) are often more cautious than males (Griffin, 2015); in addition, elderly cyclists typically exhibit slower kinematics compared to young cyclists (Vlakveld et al., 2015). Finally, of course, poor visibility and low friction would elicit a more cautious behaviour which, in the case of braking, would most likely result in an earlier start of a smoother braking manoeuvre.

Steering appeared to be a more complex manoeuvre than braking since it could not be described with a single parameter, although variability (in our model parameters) was larger for braking than for steering across the participants. The Gaussian curve model we propose captures the main characteristics of a steering manoeuvre with the following four features: 1) lateral displacement (amplitude of the

Gaussian), 2) starting point in relation to the obstacle (μ-2σ), 3) extension (standard deviation), and 4) cyclist offset (to what extent the cyclist came back to the same lateral position on the road after the manoeuvre). The amplitude and standard deviation of our Gaussian model can inform the design of infrastructure by describing how much manoeuvring space cyclists need for comfortably overtaking other cyclists. Specifically, our model suggests that overtaking a stady cyclist may require apporximately 1 m and 10 m in the longitudinal and lateral direction, respectively. Additionally, the model's mean and standard deviation are important parameters for active safety, since they describe the point when a cyclist initiates a steering manoeuvre to comfortably avoid an obstacle.

As speed increases, steering may occur later than braking (shorter time to collision and closer to the obstacle), without compromising comfort—suggesting that, as for cars (Brännström et al., 2014), steering
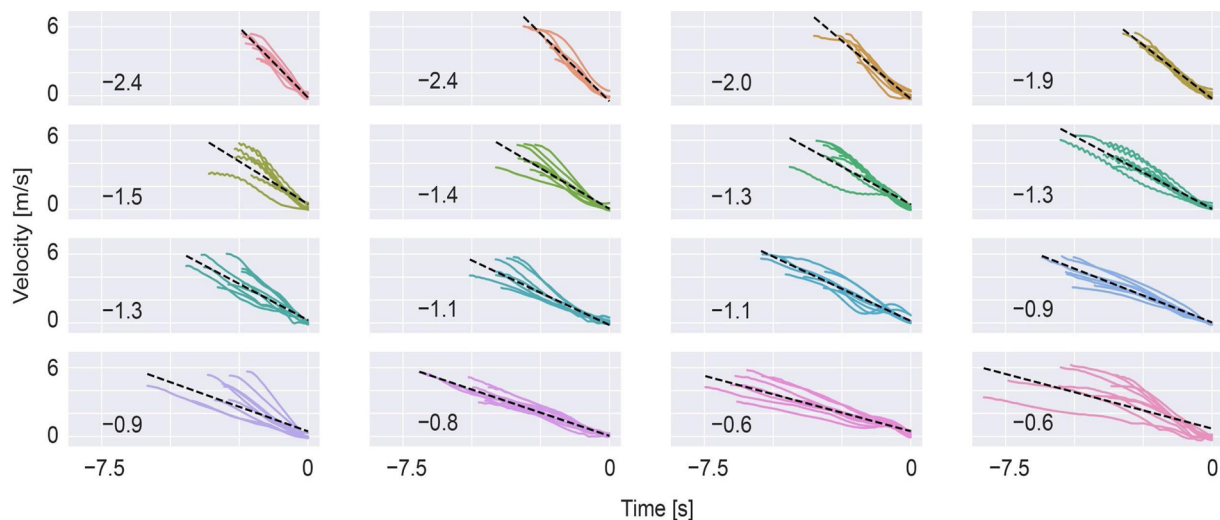

Fig. 6. Speed profiles during braking and linear braking models (dashed line) for the 16 individual participants. The slope of the model, which represents the braking acceleration in m/s^2, is presented in the lower left of each subfigure.
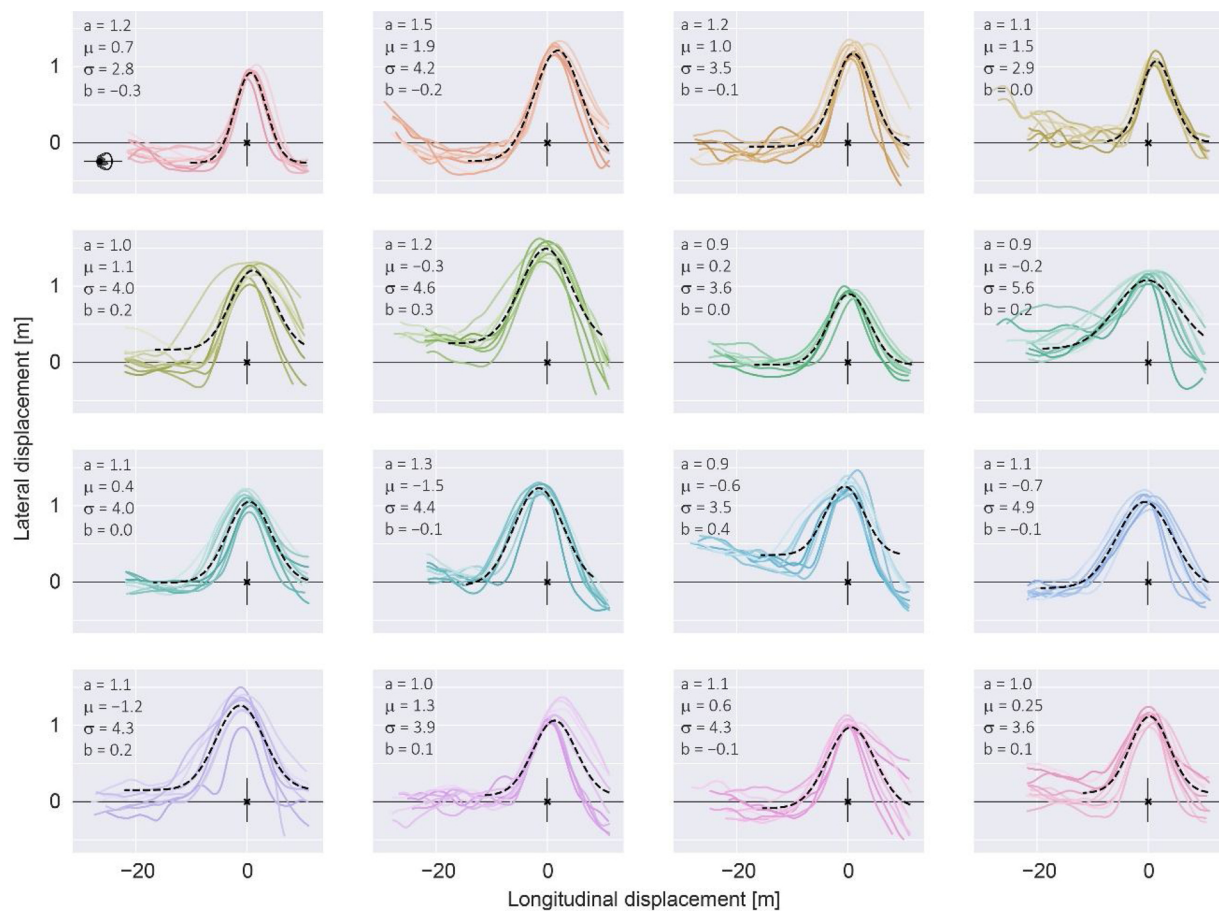
Fig. 7. Bird's-eye view of the steering manoeuvres for the 16 participants. The dummy cyclist (represented with a small cross) is located at the origin of the axes, and the vertical line indicates its width. An icon of the participant is only represented in the top-left panel. The coloured lines show the trajectory of each cyclist as she approached the dummy cyclist and circumvented it. The Gaussian model for each participant is also presented (dashed line) with the model parameters; all parameters in the Gaussian model are in meters.

may be a more effective avoidance manoeuvre when a threat is imminent (and enough lateral clearance is available). In other words, unlike braking manoeuvres, steering manoeuvres do not require more longitudinal distance as driving speed increases, although the latter need to consider lateral clearance, which the former does not. As a consequence, steering may become the more comfortable manoeuvre as speed increases and/or distance to the obstacle decreases. Therefore, in *unplanned* avoidance manoeuvres (i.e. situations where a cyclist is unexpectedly required to avoid a conflict, as opposed to the protocol in studies where cyclists knew ahead of time when and where they would have needed to avoid an obstacle (Huertas-Leyva et al., 2019)), steering away may be the most comfortable (and possibly safe) manoeuvre if the infrastructure allows for it and stability is not at stake.

Altogether, the parameters from both models presented in this paper may enable active safety systems to predict cyclists' intention to steer or brake—if a cyclist approaches another from behind, she may steer away; or if she approaches an intersection, she may brake (Boda et al., 2018). Current active safety systems support drivers overtaking cyclists, as well as drivers avoiding crashing with cyclists at intersections (Euro NCAP, 2017); however, these systems do not integrate models for cyclist braking and steering such as the ones presented in this paper. Rating programs such as Euro NCAP could also use the results from this paper, and the braking model specifically, in the design of realistic test conditions, such as those developed by (Den Camp et al., 2017) in which automated emergency systems may intervene if cyclists do not stop at intersections. In addition, the models presented in this paper can support virtual assessment using counterfactual simulations (Bärgman et al., 2017).

Individual variability in steering manoeuvres was, as in braking manoeuvres, larger across participants than across speed conditions for individual participants. The cyclist variability was lower in the steering manoeuvre than in the braking manoeuvre, possibly because of bicycle dynamics (Schwab and Meijaard, 2013). Of course, variability will further increase as new demographic and environmental factors will come into play, and future research should determine which factors are most important to consider.

This study is a first step in modelling cyclist-avoidance manoeuvres to inform active safety and infrastructure design; as such, it provides some ballpark figures that can support 1) calculations for threat assessment algorithms and 2) test design for active safety. Active safety systems, such as automated braking, promise to avoid collisions with cyclists, are currently part of Euro NCAP and may become mandatory in the near future (Van Ratingen et al., 2016). The results of this paper suggest for Euro NCAP to use constant deceleration for the cyclist's dummy, when testing automated braking in intersection scenarios with a cyclist (Euro NCAP, 2017). In addition, our models may help automated vehicles interact with cyclists at intersections by predicting cyclists' intent to yield as they approach an intersection (Sandt and Owens, 2017; Vissers et al., 2017). Finally, the steering models from this paper may inform infrastructure design by explaining how much space (laterally and longitudinally) a cyclist needs for overtaking. Because of the introduction of small electric vehicles for personal mobility (such as pedelecs, electric scooters, etc.), overtaking manoeuvres are a growing concern for cycling safety (Dozza and Bianchi-Piccinini, 2014), and may require some infrastructure to be redesigned.

This paper introduced cyclist comfort zone by borrowing from

driver behaviour literature. Although a bicycle constrains locomotion differently than a motorised vehicle, concepts such as the field of safe travel and minimum stopping distance (Gibson and Crooks, 1938) are as easy to apply to cyclists as to drivers. The field of safe travel assumes that drivers create a model which indicates where they can move safely without interfering with other road users or the infrastructure. This model may include their expectations about what their vehicle kinematics can achieve (Clark, 2012; Engström et al., 2018; Papakostopoulos et al., 2017). As with a driver's field of safe travel, that of a cyclist depends on the infrastructure and the presence of other road users; however, cyclists are also challenged by balancing the bicycle (Meijaard et al., 2007), a task that further constrains their field of safe travel due to the additional requirements of lateral space for balance. A cyclist's comfort zone is also affected by the balancing task, and consequently, by bicycle type and the extent to which the cyclist is acquainted with the balancing task. Finally, cyclists need to propel the bicycle (typically by pedalling). To prioritise or facilitate the balancing and manoeuvring tasks, pedalling may be interrupted; at times, however, it becomes urgent (to support the balancing task) and cannot be interrupted. In these critical situations, pedalling is an additional constraint on the comfort zone. Steering a bicycle differs from braking in that it requires less physical energy (no need to re-accelerate), does not require as much space, and is seldom regulated by the infrastructure. Therefore, a *minimum steering zone* (i.e. the minimum lateral distance required to complete a manoeuvre) may be more relevant to a cyclist than to a driver for defining her comfort zone or field of safe travel (Gibson and Crooks, 1938).

In this study, we modelled the comfort zone based on the behaviour that sixteen cyclists exhibited while performing braking and steering tasks, according to the instruction from a test leader in an isolated urban area. We assumed cyclists behaved naturally because we asked them to do so. Nevertheless, the lack of a real traffic environment and the experimental protocol may have influenced the cyclist behaviour, for instance, discouraging self-sufficing behaviours (Summala, 2007). Further, to preserve the participants' safety, we controlled the environment (e.g. no other road-user was present, data were not collected in adverse weather conditions, etc.) which may have, to some extent, compromised the ecological validity of the data. In addition, because of the experimental protocol, all avoidance manoeuvres were planned (i.e. they were expected to happen at a specific time and place). While such situations are common in traffic, for instance as a cyclist approaches an intersection with a red light, planned manoeuvres have been shown to exhibit milder kinematics than unplanned manoeuvres (Huertas-Leyva et al., 2019). Although this study used common bicycles, the extent to which our results would transfer to other types of bicycles should be addressed in future studies. Bicycles may have very different geometry and braking systems that may constrain and influence cyclist's behaviour (Huertas-Leyva et al., 2018). Particularly interesting may be e-bicycles (pedelecs) that have shown to elicit different riding behaviour than traditional bicycles (Cherry Weinert and Xinmiao, 2009; Dozza et al., 2015; Schleinitz et al., 2017; Vlakveld et al., 2015; Wu et al., 2012). Also, in this study, we used a dummy cyclist as an obstacle; while this solution was easy to implement and safe, it may not be representative of other obstacles, such as water puddles and potholes in the ground, that are usually circumvented by cyclists. Finally, because of our small sample, we are not able to determine the extent to which demographic factors, such as gender and age, may affect our results. In conclusion, the models presented in this paper may not be representative of the actual comfort zone of cyclists in traffic for all situations, a limitation shared by all studies, to one degree or another, that model human behaviour from controlled studies. Modelling comfort zone using naturalistic data (Dozza and Werneke, 2014), may be a sounder approach because of the high ecological validity of such data; however, today these datasets are too small to derive usable models. In fact, previous studies have shown how the large variability from the environment in small naturalistic cycling studies may transfer to the

models, making their predictions imprecise and therefore of little help (Dozza and Fernandez, 2014).

Future studies may overcome some of the current limitations by 1) testing different types of bicycles and brakes, 2) including a wider range of cyclists (e.g. different demographics), 3) including different and moving obstacles, 4) verifying the extent to which the models change as the avoidance manoeuvres become more urgent, unexpected, and critical, 5) evaluating the extent to which braking and steering are affected by environmental factors such as road friction and visibility, and 6) use naturalistic data (once they will be available in large quantity). Finally, this paper exemplifies how to use cyclist behaviour models for active safety and infrastructure design; however, these models may also be used in driving (or riding) simulators and multi-agent traffic simulations to make sure cyclists behave in these virtual worlds as they would in reality.

5. Conclusions

This paper presented a framework that leveraged the literature on driver behaviour to operationalise cyclist comfort zone in objective terms, by measuring and modelling cyclist manoeuvres. We introduced two models that quantitatively describe cyclist behaviour in comfortable obstacle avoidance: one for braking and one on steering. We also exemplified how these models can support active safety and infrastructure design as well as assessment protocols for new products. Because new e-vehicles for personal mobility are increasingly common and automated vehicles promise to soon enter the traffic system, this framework may be useful to assess the safety of the new modal split and of the new interactions among road users.

While most of the literature on driver behaviour and comfort zones may apply to cyclists as well, the extra balancing and pedalling tasks while cycling may require that some results from driving safety research be extended with additional research specifically addressing cyclists. This is an important difference that deserves further research to understand how cyclists adapt their field of safe travel depending on their need to trade between keeping the bicycle stable and fulfilling their mobility goals. Future studies should also investigate the extent to which braking and steering models change as cyclists are exposed to increasingly critical and unexpected situations so that not only the comfort zone but also the safety margins for cycling can be objectively quantified.

CRediT authorship contribution statement

Oliver Lee: Methodology, Software, Validation, Formal analysis, Investigation, Data curation, Visualization, Writing - original draft. **Alexander Rasch:** Investigation, Visualization, Writing - review & editing. **Arend L. Schwab:** Formal analysis, Resources, Supervision, Project administration, Funding acquisition, Writing - review & editing. **Marco Dozza:** Conceptualization, Methodology, Formal analysis, Resources, Visualization, Supervision, Project administration, Funding acquisition, Writing - review & editing.

Declaration of Competing Interest

The authors declare that they have no known competing financial interests or personal relationships that could have appeared to influence the work reported in this paper.

Acknowledgements

References

Bärgman, J., 2016. Methods for Analysis of Naturalistic Driving Data in Driver Behavior Research.

Bärgman, J., Boda, C.N., Dozza, M., 2017. Counterfactual simulations applied to SHRP2 crashes: the effect of driver behavior models on safety benefit estimations of intelligent safety systems. Accid. Anal. Prev. https://doi.org/10.1016/j.aap.2017.03.003.

Bärgman, J., Smith, K., Werneke, J., 2015. Quantifying drivers' comfort-zone and dread-zone boundaries in left turn across path/opposite direction (LTAP/OD) scenarios. Transp. Res. Part F Traffic Psychol. Behav. 35, 170–184.

Bhatia, R., Wier, M., 2011. Safety in Numbers" re-examined: Can we make valid or practical inferences from available evidence? Accid. Anal. Prev. 43 (1), 235–240. https://doi.org/10.1016/j.aap.2010.08.015.

Boda, C.-N., 2019. Driver Interaction With Vulnerable Road Users Modelling Driver Behaviour in Crossing Scenarios. Chalmers University of Technology. https://www.researchgate.net/profile/Christian-Nils_Boda/publication/337544513_Driver_interaction_with_vulnerable_road_users_Modelling_driver_behaviour_in_crossing_scenarios/links/5ddd400f299bf10bc327fcae/Driver-interaction-with-vulnerable-road-users-Mode.

Boda, C.-N., Dozza, M., Bohman, K., Thalya, P., Larsson, A., Lubbe, N., 2018. Modelling how drivers respond to a bicyclist crossing their path at an intersection: How do test track and driving simulator compare? Accid. Anal. Prev. 111. https://doi.org/10.1016/j.aap.2017.11.032.

Brannstrom, M., Coelingh, E., Sjoberg, J., 2010. Model-based threat assessment for avoiding arbitrary vehicle collisions. Ieee Trans. Intell. Transp. Syst. 11 (3), 658–669. https://doi.org/10.1109/Tits.2010.2048314.

Brännström, M., Coelingh, E., Sjöberg, J., 2014. Decision-making on when to brake and when to steer to avoid a collision. International Journal of Vehicle Safety 1 7 (1), 87–106.

Brezina, E., Krämer, M., 1970. An investigation of rider, bicycle, and environmental variables in urban bicycle collisions. Proceedings: American Association for Automotive Medicine Annual Conference 14, 139–165.

Cherry Weinert, J.X., Xinmiao, Y., 2009. Comparative environmental impacts of electric bikes in China. Transportation Research Part D-Transport and Environment 14 (5), 281–290. https://doi.org/10.1016/j.trd.2008.11.003.

Clark, A., 2012. Dreaming the whole cat: Generative models, predictive processing, and the enactivist conception of perceptual experience. Mind 121 (483), 753–771.

Damasio, A., Damasio, Antonio R., 1995. Descartes' error: emotion, reason, and the human brain. Relat. Ind. Vol. 50 (2). https://doi.org/10.7202/051028ar.

Den Camp, O.O., van Montfort, S., Uittenbogaard, J., Welten, J., 2017. Cyclist target and test setup for evaluation of cyclist-autonomous emergency braking. Int. J. Automot. Technol. 18 (6), 1085–1097.

Dozza, M., Bianchi-Piccinini, G., 2014. Do cyclists on e-bikes behave differently than cyclists on traditional bicycles? In: Proceedings of the 3rd International Cycling Safety Conference. Nov 18-19, Göteborg, Sweden.

Dozza, M., Bianchi-Piccinini, G., Werneke, J., 2015. Using naturalistic data to assess e-cyclist behavior. Transp. Res. Part F Traffic Psychol. Behav.

Dozza, M., Fernandez, A., 2014. Understanding bicycle dynamics and cyclist behavior from naturalistic field data (November 2012). Ieee Trans. Intell. Transp. Syst. 15 (1). https://doi.org/10.1109/TITS.2013.2279687.

Dozza, M., Hubbard, M., Schwab, A.L., 2018. Cycling safety. J. Safety Res. 67, 125.

Dozza, M., Schindler, R., Bianchi-Piccinini, G., Karlsson, J., 2016. How do drivers overtake cyclists? Accid. Anal. Prev. https://doi.org/10.1016/j.aap.2015.12.008.

Dozza, M., Werneke, J., 2014. Introducing naturalistic cycling data: What factors influence bicyclists' safety in the real world? Transp. Res. Part F Traffic Psychol. Behav. 24, 83–91.

Elvik, R., 2009. The non-linearity of risk and the promotion of environmentally sustainable transport. Accid. Anal. Prev. 41 (4), 849–855. https://doi.org/10.1016/j.aap.2009.04.009.

Engström, J., Bärgman, J., Nilsson, D., Seppelt, B., Markkula, G., Piccinini, G.B., Victor, T., 2018. Great expectations: a predictive processing account of automobile driving. Theor. Issues Ergon. Sci. https://doi.org/10.1080/1463922X.2017.1306148.

Euro NCAP, 2017. European New Car assessment (Euro NCAP) - Test Protocol AEB VRU Systems (Issue Version 2.0).

Fuller, R., 1984. A conceptualization of driving behaviour as threat avoidance. Ergonomics 27 (11), 1139–1155. https://doi.org/10.1080/00140138408963596.

Gibson, J.J., Crooks, L.E., 1938. A theoretical field-analysis of automobile-driving. Am. J. Psychol. 51 (3), 453–471.

Griffin, W.M., 2015. Male and Female, Cyclist and Driver Perceptions of Crash Risk in Critical Road Situations. Queensland University of Technology. https://eprints.qut.edu.au/81817/.

Gustafsson, P., Dozza, M., Lindgren, L., Boda, C.-N., Muñoz-Cantillo, J.C., 2013. BikeCOM – A cooperative safety application supporting cyclists and drivers at intersections. Proceedings of the 3rd Conference of Driver Distraction and Inattention. Gothenbrug 2013 (4-6 September), 1–16. http://publications.lib.chalmers.se/publication/174772-bikecom-a-cooperative-safety-application-supporting-cyclists-and-drivers-at-intersections.

Hudson, M., 1978. The Bicycle Planning Book.

Huertas-Leyva, P., Dozza, M., Baldanzini, N., 2018. Investigating cycling kinematics and braking maneuvers in the real world: e-bikes make cyclists move faster, brake harder, and experience new conflicts. Transp. Res. Part F Traffic Psychol. Behav. 54. https://doi.org/10.1016/j.trf.2018.02.008.

Huertas-Leyva, P., Dozza, M., Baldanzini, N., 2019. E-bikers' braking behavior: results from a naturalistic cycling study. Traffic Inj. Prev. 1–6.

Johnson, M., Charlton, J., Oxley, J., Newstead, S., 2010. Naturalistic cycling study: identifying risk factors for on-road commuter cyclists. Ann. Adv. Automot. Med. 54, 275–283.

Lübbe, N., 2015. Integrated Pedestrian Safety Assessment: A Method to Evaluate Combinations of Active and Passive Safety.

Meijaard, J.P., Papadopoulos, J.M., Ruina, A., Schwab, A.L., 2007. Linearized dynamics equations for the balance and steer of a bicycle: a benchmark and review. Proceedings of the Royal Society A: Mathematical, Physical and Engineering Sciences 463 (2084), 1955–1982.

Näätänen, R., Summala, H., 1974. A model for the role of motivational factors in drivers' decision-making*. Accid. Anal. Prev. 6 (3–4), 243–261. https://doi.org/10.1016/0001-4575(74)90003-7.

Papakostopoulos, V., Marmaras, N., Nathanael, D., 2017. The "field of safe travel" revisited: interpreting driving behaviour performance through a holistic approach. Transp. Rev. 37 (6), 695–714. https://doi.org/10.1080/01441647.2017.1289992.

Sandt, L., Owens, J.M., 2017. Discussion Guide for Automated and Connected Vehicles, Pedestrians, and Bicyclists.

Schepers, P., Twisk, D., Fishman, E., Fyhri, A., Jensen, A., 2017. The Dutch road to a high level of cycling safety. Saf. Sci. 92, 264–273.

Schleinitz, K., Petzoldt, T., Franke-Bartholdt, L., Krems, J., Gehlert, T., 2017. The German Naturalistic Cycling Study – comparing cycling speed of riders of different e-bikes and conventional bicycles. Saf. Sci. 92, 290–297. https://doi.org/10.1016/j.ssci.2015.07.027.

Schwab, A.L., Meijaard, J.P., 2013. A review on bicycle dynamics and rider control. Veh. Syst. Dyn. 51 (7), 1059–1090. https://doi.org/10.1080/00423114.2013.793365.

Schwab, A.L., Meijaard, J.P., 2017. Determining the necessary width of a bicycle lane by means of simulations on a bicycle-rider model. The 6th International Cycling Safety Conference (September).

Summala, H., 2007. Towards understanding motivational and emotional factors in driver behaviour: comfort through satisficing. In: Cacciabue, P.C. (Ed.), Modelling Driver Behaviour in Automotive Environments. Springer, London, pp. 189–207. https://doi.org/10.1007/978-1-84628-618-6_11.

Vaa, T., 2014. From Gibson and Crooks to Damasio: The role of psychology in the development of driver behaviour models. Transp. Res. Part F Traffic Psychol. Behav. 25, 112–119. https://doi.org/10.1016/j.trf.2014.02.004.

Van Ratingen, M., Williams, A., Lie, A., Seeck, A., Castaing, P., Kolke, R., Adriaenssens, G., Miller, A., 2016. The European New Car Assessment Programme: A historical review. Chinese Journal of Traumatology - English Edition 19 (2), 63–69. https://doi.org/10.1016/j.cjtee.2015.11.016.

Vissers, L.K., van der Schagen, S., van, I.N.L.G., Hagenzieker, M.P., 2017. Safe Interaction Between Cyclists, Pedestrians and Automated Vehicles: What Do We Know and What Do We Need to Know?.

Vlakveld, W.P., Twisk, D., Christoph, M., Boele, M., Sikkema, R., Remy, R., Schwab, A.L., 2015. Speed choice and mental workload of elderly cyclists on e-bikes in simple and complex traffic situations: a field experiment. Accid. Anal. Prev. 74, 97–106. https://doi.org/10.1016/j.aap.2014.10.018.

Wu, C.X., Yao, L., Zhang, K., 2012. The red-light running behavior of electric bike riders and cyclists at urban intersections in China: An observational study. Accid. Anal. Prev. 49, 186–192. https://doi.org/10.1016/j.aap.2011.06.001.